Article

Optical Recognition of Surface Chirality at Au(*hkl*) Single Crystalline Surfaces by Second Harmonic Generation Rotational Anisotropy

Ichizo Yagi, Masaki Chiba, and Kohei Uosaki

J. Am. Chem. Soc., **2005**, 127 (36), 12743-12746• DOI: 10.1021/ja053724p • Publication Date (Web): 18 August 2005

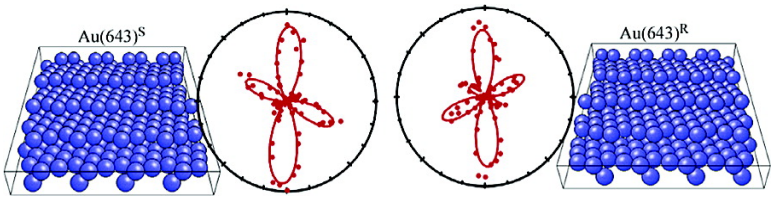

J|A|C|S
ARTICLES
Published on Web 08/18/2005

Optical Recognition of Surface Chirality at Au(*hkl*) Single Crystalline Surfaces by Second Harmonic Generation Rotational Anisotropy

Ichizo Yagi,*[,†,‡] Masaki Chiba,[†] and Kohei Uosaki[†]

Contribution from the Physical Chemistry Laboratory, Division of Chemistry, Graduate School of Science, Hokkaido University, N10W8 Kita-ku, Sapporo 060-0810, Japan, and PRESTO, Japan Science and Technology Agency, Kawaguchi 332-0012, Japan

Received June 7, 2005; E-mail: yagi@pchem.sci.hokudai.ac.jp

Abstract: Two-dimensional chirality at naturally chiral gold single crystalline surfaces was detected and characterized using optical second harmonic generation (SHG) measurements. SHG rotational anisotropy (SH-RA) patterns at Au(643)^S and Au(643)^R surfaces were mirror symmetric to each other. Systematic SH-RA measurements at chiral Au(*hkl*) surfaces with the same step and kink structures but different (111) terrace widths showed a linear correlation between surface step density and SH-RA fitting parameters arising from defects. These results indicate that SH-RA measurements provide information not only on surface chirality but also on density of surface defects.

Introduction

The chirality of molecules is critical in biological and organic chemical systems. In addition to traditional interests in recognition, separation, and synthesis of enantiomers, interest has recently been shown in two-dimensional chirality because chiral recognition at surfaces plays an important role in various processes such as chiral chromatography,[1] anisotropic crystal growth,[2,3] chiral sensing,[4−6] and heterogeneous asymmetric catalysis.[7−9] Although two-dimensional chirality has been mainly achieved by formation of chiral molecular layers on solid surfaces,[10−13] solid surfaces with chiral crystallographic orientation (i.e., naturally chiral surfaces)[14−19] have been also developed to investigate the two-dimensional chiral processes.

Naturally chiral metal surfaces[14−19] have periodical kink sites, and the handedness of the kink microstructure governs the overall chirality of the crystal surface. High Miller index surfaces of pure metal surfaces such as Ag(643) and Pt(531) have been prepared, and enantiospecific adsorption and subsequent catalytic or electrochemical reactions of chiral molecules at these surfaces have been reported. On the other hand, chirality of such surfaces has been indirectly confirmed by limited methods, such as differences in electrochemical (EC)[15,17,20] or temperature-programmed desorption (TPD)[14,21] responses for chiral reactants, but these methods are not quantitative. While direct determination of surface structure is possible by using electron spectroscopic methods under ultrahigh vacuum (UHV) such as low-energy electron diffraction (LEED),[14,20] these methods are not suitable for monitoring interfacial chiral recognition processes in situ. Chiral recognition processes at two-dimensional chiral systems have been achieved by scanning probe microscopes (SPMs) at atomic or molecular scale only under UHV,[10] although chiral molecular layer formation has been confirmed even at the solid/liquid interface by SPMs.[11,12] Optical methods might be an ideal tool for monitoring chiral recognition processes quantitatively in situ. However, a linear optical method provides small sensitivity for chirality even in condensed chiral media, and more sensitive optical probes are required for chiral surfaces and interfaces, where extremely smaller number of atoms or molecules contribute to the signal.[22]

† Hokkaido University.
‡ Japan Science and Technology Agency.

(1) Beesley, T. E.; Scott, R. P. W. *Chiral Chromatography*; Wiley & Sons: Chichester, U.K., 2000; Vol. 18, p 205.
(2) Switzer, J. A.; Kothari, H. M.; Poizot, P.; Nakanishi, S.; Bohannan, E. W. *Nature* **2003**, *425* (6957), 490.
(3) Bohannan, E. W.; Kothari, H. M.; Nicic, I. M.; Switzer, J. A. *J. Am. Chem. Soc.* **2004**, *126* (2), 488.
(4) Nakanishi, T.; Yamakawa, N.; Asahi, T.; Shibata, N.; Ohtani, B.; Osaka, T. *Chirality* **2004**, *16* (Suppl.), S36.
(5) Mei, X.; Wolf, C. *J. Am. Chem. Soc.* **2004**, *126* (45), 14736.
(6) Junxiang, H.; Sato, H.; Umemura, Y.; Yamagishi, A. *J. Phys. Chem. B* **2005**, *109* (10), 4679.
(7) Noyori, R. *Chemtech* **1992**, *22* (6), 360.
(8) Baiker, A. *J. Mol. Catal. A: Chem.* **1997**, *115* (3), 473.
(9) Sholl, D., Gellman, A., Eds.; Special Issue: Heterogeneous Chiral Catalysis. *J. Mol. Catal. A: Chem.* **2004**, *216* (2), 165−294.
(10) Humblot, V.; Barlow, S. M.; Raval, R. *Prog. Surf. Sci.* **2004**, *76*, 1.
(11) Feyter, S. D.; De Schryver, F. C. *Chem. Soc. Rev.* **2003**, *32*, 139.
(12) Ohtani, B.; Shintani, A.; Uosaki, K. *J. Am. Chem. Soc.* **1999**, *121* (27), 6515.
(13) Barlow, S. M.; Raval, R. *Surf. Sci. Rep.* **2003**, *50*, 201.
(14) McFadden, C. F.; Cremer, P. S.; Gellman, A. J. *Langmuir* **1996**, *12* (10), 2483.
(15) (a) Ahmadi, A.; Attard, G.; Feliu, J.; Rodes, A. *Langmuir* **1999**, *15* (7), 2420. (b) Attard, G. A. *J. Phys. Chem. B* **2001**, *105* (16), 3158.
(16) Sholl, D. S.; Asthagiri, A. R.; Power, T. D. *J. Phys. Chem. B* **2001**, *105* (21), 4771.
(17) Attard, G. A.; Harris, C.; Herrero, E.; Feliu, J. *Faraday Discuss.* **2002**, *121*, 253.
(18) Horvath, J. D.; Gellman, A. J.; Sholl, D. S.; Power, T. D. In *Chirality: Physical Chemistry*; Hicks, J. M., Ed.; ACS Symposium Series 810; American Chemical Society: Washington, DC, 2002; p 269.
(19) Horvath, J. D.; Gellman, A. J. *Top. Catal.* **2003**, *25* (1−4), 9.
(20) Attard, G. A.; Ahmadi, A.; Feliu, J.; Rodes, A.; Herrero, E.; Blais, S.; Jerkiewicz, G. *J. Phys. Chem. B* **1999**, *103* (9), 1381.
(21) Horvath, J. D.; Koritnik, A.; Kamakoti, P.; Sholl, D. S.; Gellman, A. J. *J. Am. Chem. Soc.* **2004**, *126* (45), 14988.
(22) Sioncke, S.; Verbiest, T.; Persoons, A. *Mater. Sci. Eng.* **2003**, *R42* (5−6), 115.

10.1021/ja053724p CCC: $30.25

Second-order nonlinear spectroscopies, including optical second harmonic generation (SHG)[23−27] and sum frequency generation (SFG),[22,28,29] have been known to be surface- or interface-selective optical probes, since the even-order nonlinear optical processes can occur from the break of inversion symmetry. Two-dimensional chirality is a break of inversion symmetry, and then, SHG and SFG spectroscopies become the most sensitive optical tools for chiral surfaces or interfaces. There have been many studies on applications and developments of SHG and SFG techniques for characterization of two-dimensional chirality. However, those studies concentrated on qualitative analysis of two-dimensional chirality at solid surfaces with chiral molecular layers, although a naturally chiral metal surface with an atomically ordered structure is an ideal model surface for investigating the chiral recognition processes by an optical technique. For such investigations, methods for characterizing naturally chiral metal surfaces using SHG and/or SFG spectroscopy should be systematized, and, as the first step, we applied SHG rotational anisotropy (SH-RA) measurement to quantitatively characterize a surface structure with chirality. SH-RA measurements have been extensively investigated as an optical tool for detecting the surface symmetry at the atomic level.[24,27] In the present study, SH-RA responses from naturally chiral Au single crystalline surfaces were proved to directly reflect their chirality.

Experimental Section

Au single crystalline beads were prepared using the method developed by Clavilier et al.[30] from 99.999% Au wire (Tanaka Kikinzoku). The crystal diameter was approximately 3 mm. The Au bead was oriented to the calculated directions using a reflection of He−Ne laser beam from (111) and (100) facets that appeared on the bead and was then cut and polished to be a mirror finish. The crystal was then annealed at 1073 K for 8 h to repair the damaged surface layers, and the clean, well-ordered surface was obtained by flame-annealing just before SHG measurements.

SHG measurements were performed using a tunable optical parametric oscillator (OPO) (Rambda Physics, ScanMate OPPO) pumped with the 355-nm output of a Q-switched Nd:YAG laser (Coherent, Infinity 40-100). The optical geometry was shown in other literature.[31,32] In the present study, a 580-nm fundamental wavelength was mainly used (SHG: 290 nm). The polarization combination of fundamental and SH beams was selected by achromatic polarizers, and the SH-RA patterns were measured by rotating the crystal surface about the surface normal. The SHG signal intensity was polar plotted as a function of the azimuthal angle, ϕ, which is defined as the angle between the optical incident plane and the $[\bar{1}\bar{1}2]$ axis of the (111) terrace on the surfaces (see Figure 1).

Results and Discussion

Figure 2 shows SH-RA patterns of Au(643) (upper panel in each polarization combination) and Au($\bar{6}\bar{4}\bar{3}$) (lower panel) surfaces under p-in/p-out and s-in/s-out polarization combinations as filled circles. The (643) and ($\bar{6}\bar{4}\bar{3}$) surfaces of fcc metals (structures shown in Figure 3) have been investigated as typical examples of naturally chiral surfaces and defined as $(643)^S$ and $(643)^R$ surfaces, respectively. Although the surfaces were annealed just before the SH-RA measurements, the measurements were carried out in air, and then the surface reconstruction induced by flame-annealing should be lifted. Both p-in/p-out and s-in/s-out SH-RA patterns of $Au(643)^S$ and $Au(643)^R$ surfaces are straightforward, showing inversion symmetry versus mirror plane shown as a broken line.

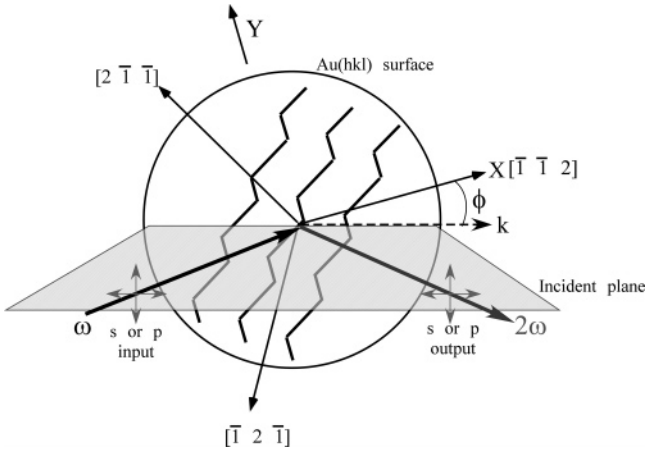

Figure 1. Experimental geometry for SH-RA measurements.

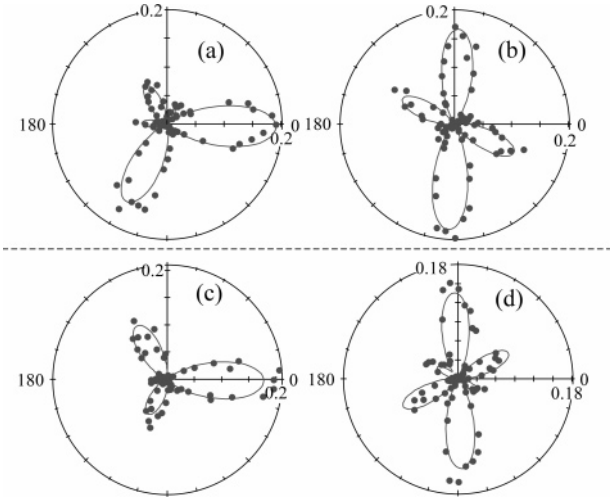

Figure 2. SH-RA patterns of (a),(b) Au(643)S and (c),(d) Au(643)R surfaces with (a),(c) p-in/p-out and (b),(d) s-in/s-out polarization combinations. Excitation of 580 nm and 290-nm detection.

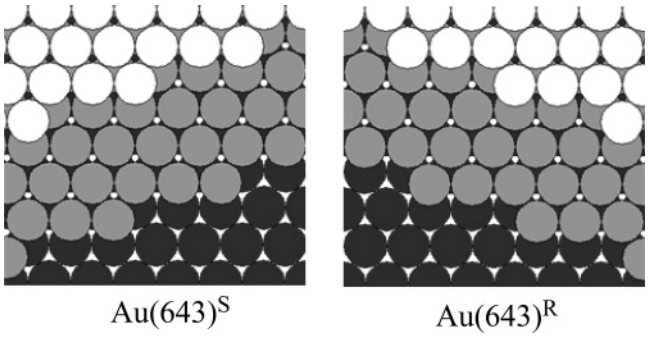

Figure 3. Surface structures of $Au(643)^S$ and $Au(643)^R$ surfaces.

(23) Shen, Y. R. *Nature* **1989**, *337* (6207), 519.
(24) Richmond, G. L.; Robinson, J. M.; Shannon, V. L. *Prog. Surf. Sci.* **1988**, *28* (1), 1.
(25) McGilp, J. F. *J. Phys. D: Appl. Phys.* **1996**, *29* (7), 1812.
(26) Heinz, T. F.; Reider, G. A. *Trends Anal. Chem.* **1989**, *8* (6), 235.
(27) Corn, R. M.; Higgins, D. A. *Chem. Rev.* **1994**, *94* (1), 107.
(28) Shen, Y. R. *Pure Appl. Chem.* **2001**, *73* (10), 1589.
(29) Simpson, G. J. *Chem. Phys. Chem.* **2004**, *5* (9), 1301.
(30) Clavilier, J.; Faure, R.; Guinet, G.; Durand, R. *J. Electroanal. Chem.* **1980**, *107*, 205.
(31) Awatani, T.; Yagi, I.; Noguchi, H.; Uosaki, K. *J. Electroanal. Chem.* **2002**, *524*−*525*, 184.
(32) Yagi, I.; Nakabayashi, S.; Uosaki, K. *J. Phys. Chem. B* **1997**, *101* (38), 7414.

At a reconstruction-lifted Au(111) surface, the SH-RA patterns show threefold or sixfold symmetric patterns depending on the input/output polarization combinations and fundamental/SH wavelengths. Such SH-RA patterns at the Au(111) surface correspond to C_{3v} symmetry by considering the topmost and second layers and are fitted by the following equations:

$$I(2\omega)^{pp,sp} = |\mathbf{a}^{(\infty)} + \mathbf{d}^{(3)} \cos(3\phi)|^2 I(\omega)^2 \quad (1a)$$

$$I(2\omega)^{ps,ss} = |\mathbf{d}^{(3)'} \sin(3\phi)|^2 I(\omega)^2 \quad (1b)$$

where the superscripts on the left-hand sides denote the polarization conditions of pp- (p-in/p-out) and sp- or ps- and ss-polarization combinations; $\mathbf{a}^{(\infty)}$, $\mathbf{d}^{(3)}$, and $\mathbf{d}^{(3)\prime}$ are the amplitudes of the isotropic ($\mathbf{a}^{(\infty)}$) and threefold ($\mathbf{d}^{(3)}$ and $\mathbf{d}^{(3)\prime}$) symmetry contributions, respectively; and $I(\omega)$ is the incident laser intensity. These amplitude terms are the products of Fresnel factors and tensor elements of second-order nonlinear susceptibility, $\chi^{(2)}$, depending on the surface symmetry and polarization combination, and $\mathbf{a}^{(\infty)}$, $\mathbf{d}^{(3)}$, and $\mathbf{d}^{(3)\prime}$ are complex values. For C_{3v} symmetry, there are four nonzero tensor elements of $\chi^{(2)}$, that is, $\chi^{(2)}_{zzz}$, $\chi^{(2)}_{zxx}$, $\chi^{(2)}_{xxz}$, and $\chi^{(2)}_{xxx}$ (see refs 33 and 34 for details of $\chi^{(2)}$ tensor.). Since the decline in surface symmetry causes an increase in the number of nonzero $\chi^{(2)}$ tensor elements, the introduction of periodic anisotropic defects on the Au(111) surface deforms the SH-RA patterns from symmetric threefold or sixfold patterns.

Richmond and co-workers have shown that the SH-RA pattern is deformed by an introduction of periodic atomic step lines on a Ag(111) surface.[35,36] The introduction of periodic step lines converts a sixfold symmetric pattern to a twofold symmetric one. In the case of a (643) surface, further introduction of periodic kink sites on step lines reduces the overall symmetry to C_s. However, as is shown in Figures 2 and 3, the overall C_s symmetry at Au(643) and Au($\bar{6}43$) surfaces can be interpreted as a result of superimposition of C_{2v} and C_s symmetries on C_{3v} symmetry of Au(111) substrates. Thus, we applied the following equations to fit the SH-RA patterns in Figure 2 by adding C_s and C_{2v} terms in eqs 1:

$$I(2\omega)^{pp,sp} = |\mathbf{a}^{(\infty)} + \mathbf{b}^{(1)} \cos(\phi + \alpha_1) + \mathbf{c}^{(2)} \cos(2\phi + \alpha_2) + \mathbf{d}^{(3)} \cos(3\phi)|^2 I(\omega)^2 \quad (2a)$$

$$I(2\omega)^{ps,ss} = |\mathbf{b}^{(1)'} \sin(\phi + \alpha_1) + \mathbf{c}^{(2)'} \sin(2\phi + \alpha_2) + \mathbf{d}^{(3)'} \sin(3\phi)|^2 I(\omega)^2 \quad (2b)$$

where $\mathbf{b}^{(1)}$, $\mathbf{c}^{(2)}$, and $\mathbf{b}^{(1)\prime}$, $\mathbf{c}^{(2)\prime}$ are the amplitudes of the onefold and twofold symmetry contributions for pp- (p-in/p-out) and sp- or ps- and ss-polarization combinations, respectively. The **b** and **c** terms can be understood arising from the symmetric break by kink and step sites, and the offset angles of α_1 and α_2 relative to the [$\bar{1}$12] direction of the surface can be correlated to the crystallographic orientation on the surface. These equations resemble the fitting equations for a single crystalline Au(110) surface,[37] where the microfacetting induced by the surface reconstruction makes the overall symmetry from C_{2v} to C_s by the superimposing C_s and C_{3v} symmetry contributions.

Table 1. Fitting Parameters for SH-RA Patterns in Figure 2 by Eqs 2a,b

		$\lvert\mathbf{a}^{(\infty)}\rvert$	$\lvert\mathbf{b}^{(1)}\rvert$	$\lvert\mathbf{c}^{(2)}\rvert$	$\lvert\mathbf{d}^{(3)}\rvert$	α_1	α_2
$(643)^S$	p/p	0.1195	0.1287	0.0652	0.2368	43.41°	−49.11°
	s/s	−	0.2062	0.0313	0.2814		
$(643)^R$	p/p	0.116	0.1049	0.0901	0.229	−43.41°	49.11°
	s/s	−	0.1685	0.0138	0.2716		

The results obtained by fitting with eqs 2a,b are shown in Figure 2 as solid lines. Fitting parameters are shown in Table 1. It should be noted that the fixed value of the offset angle, α_1, is the most effective for the fitting and was assumed to be 43.4°, which corresponds to the angle between the [$\bar{1}$12] direction and the cutting direction to prepare the $(643)^{R/S}$ surface. The magnitude of $\mathbf{b}^{(1)}$ is comparable to that of $\mathbf{d}^{(3)}$, while the magnitude of $\mathbf{c}^{(2)}$ seems to be 10 times smaller than that of $\mathbf{d}^{(3)}$. Thus, the superimposition of C_s symmetry mainly contributes to the deformation of SH-RA patterns.

To examine the validity of our fitting equations and verify the assumption for the offset angle α_1, SH-RA measurements were performed at three pairs of chiral surfaces: Au(11 8 3)$^{R/S}$, Au(15 12 7)$^{R/S}$, and Au(20 17 12)$^{R/S}$ surfaces. These surfaces have the same step and kink structures, while the distance between each step line becomes larger in the order of (11 8 3) < (15 12 7) < (20 17 12) surfaces (see Supporting Information). The SH-RA patterns at these surfaces showed clear chirality as those at Au(643)$^{R/S}$ surfaces and were fitted well by eqs 2a,b as shown in Figure 4.

As the distance between each step line (i.e., the size of (111)-oriented terrace) becomes larger, the SH-RA pattern approaches the C_{3v} pattern of Au(111). The ratios $|\mathbf{a}^{(\infty)}/\mathbf{d}^{(3)}|$, $|\mathbf{b}^{(1)}/\mathbf{d}^{(3)}|$, and $|\mathbf{c}^{(2)}/\mathbf{d}^{(3)}|$ determined from fitting for p-in/p-out SH-RA patterns are plotted against the averaged step density in the cutting direction for each surface in Figure 5. Linear relations are obtained for $|\mathbf{b}^{(1)}/\mathbf{d}^{(3)}|$ and $|\mathbf{c}^{(2)}/\mathbf{d}^{(3)}|$, and these results mean that analysis of the SH-RA pattern enables evaluation of the step density even in an atomic scale. The $|\mathbf{b}^{(1)}/\mathbf{d}^{(3)}|$ ratio for Au(643)$^{R/S}$ surfaces with average step density of 1.207 nm^{-1} was 0.5 (calculated from Table 1), just located on the line in Figure 5.

Optical reflection anisotropy spectroscopy has been developed for optical recognition of chirality[38] and monatomic steps[39] at surfaces, but this method requires energy (wavelength)-resolved profiles to detect the atomic defects and the analyses are complicated. On the other hand, the SH-RA patterns reflect the two-dimensional anisotropy in the electronic polarizability around the topmost two atomic layers, which can be easily perturbed by the periodic atomic defects. The results of photoemission measurements at naturally chiral Pt surfaces by circular polarized light[40] indicated the effect of the symmetry break on the electronic polarizability in the surface, but the results in the present study seem to be more straightforward. It is noteworthy that chiral SH-RA patterns from naturally chiral

(33) Pettinger, B.; Lipkowski, J.; Mirwald, S.; Friedrich, A. *J. Electroanal. Chem.* **1992**, *329* (1−2), 289.
(34) Hirose, C.; Akamatsu, N.; Domen, K. *Appl. Spectrosc.* **1992**, *46* (6), 1051.
(35) Friedrich, K. A.; Richmond, G. L. *Chem. Phys. Lett.* **1993**, *213* (5−6), 491.
(36) Friedrich, K. A.; Richmond, G. L. *Ber. Bunsen-Ges. Phys. Chem.* **1993**, *97* (3), 386.
(37) Pettinger, B.; Mirwald, S.; Lipkowski, J. *Appl. Phys. A* **1995**, *A60* (2), 121.
(38) Macdonald, B. F.; Law, J. S.; Cole, R. J. *J. Appl. Phys.* **2003**, *93* (6), 3320.
(39) Baumberger, F.; Herrmann, T.; Kara, A.; Stolbov, S.; Esser, N.; Rahman, T. S.; Osterwalder, J.; Richter, W.; Greber, T. *Phys. Rev. Lett.* **2003**, *90* (17), 177402.
(40) Attard, G. A.; Watson, D.; Seddon, E. A.; Cornelius, S. M.; Herrero, E.; Feliu, J. *Phys. Rev. B* **2001**, *64* (11), 115408/1.

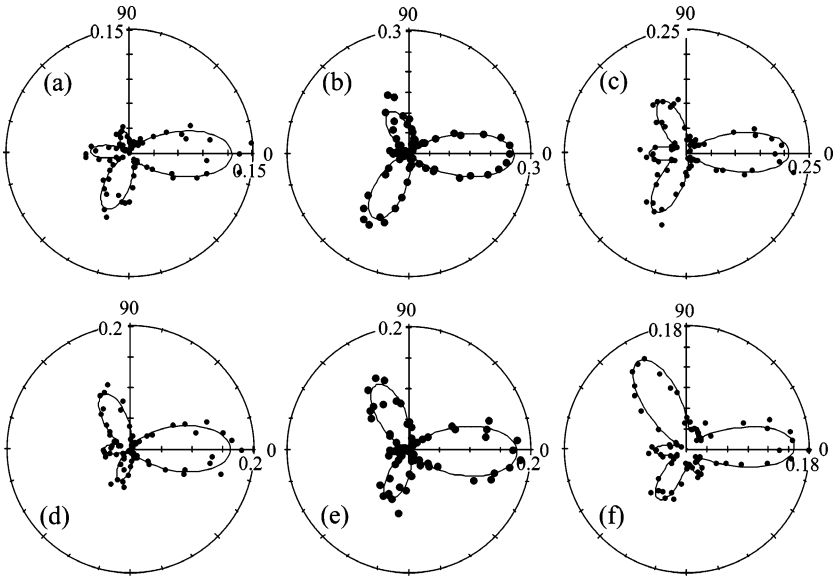

Figure 4. Step density-dependent p-in/p-out SH-RA patterns obtained at (a) Au(11 8 3)^S, (b) Au(15 12 7)^S, (c) Au(20 17 12)^S, (d) Au(11 8 3)^R, (e) Au(15 12 7)^R, (f) Au(20 17 12)^R surfaces. Excitation of 580 nm and 290-nm detection.

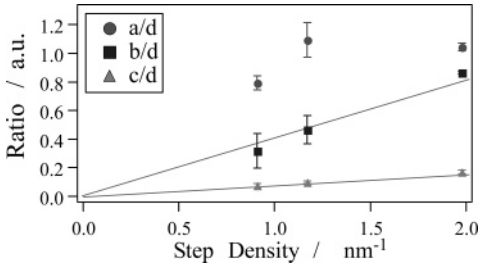

Figure 5. Step density dependence of ratios $|\mathbf{a}^{(\infty)}/\mathbf{d}^{(3)}|$, $|\mathbf{b}^{(1)}/\mathbf{d}^{(3)}|$, and $|\mathbf{c}^{(2)}/\mathbf{d}^{(3)}|$ calculated from p-in/p-out SH-RA patterns.

metal surfaces can be observed using monochromic linear-polarized light and are independent of measurement wavelength. Actually, chiral SH-RA patterns from chiral Au surfaces were clearly observed in our multicolor SHG measurements with excitation wavelengths from 550 to 640 nm and of 1064 nm (SH wavelengths from 275 to 320 nm and of 532 nm), although the shape of the SH-RA pattern depended on the excitation and SH wavelengths, as shown in Figure 6. All SH-RA patterns obtained at chiral Au surfaces were fitted with eqs 2a,b, and a contribution from C_s symmetry was reconfirmed.

In conclusion, we have demonstrated that the chirality of the interface can be recognized by the interference between the symmetry arising from the achiral substrate surface (Au(111) terrace) and the broken symmetry arising from periodic atomic defects or adsorbed molecules with constant angular offset. Although SH-RA measurements can deal with the symmetries lower than C_{3v}, it may be possible to evaluate the two-dimensional chirality at surfaces and interfaces by SH-RA method with linearly polarized light. For example, chiral surfaces formed with a monolayer of chiral molecule and an achiral Au(111) substrate can be characterized if the contribution from the molecular layer was enhanced by electronic or vibrational resonance.

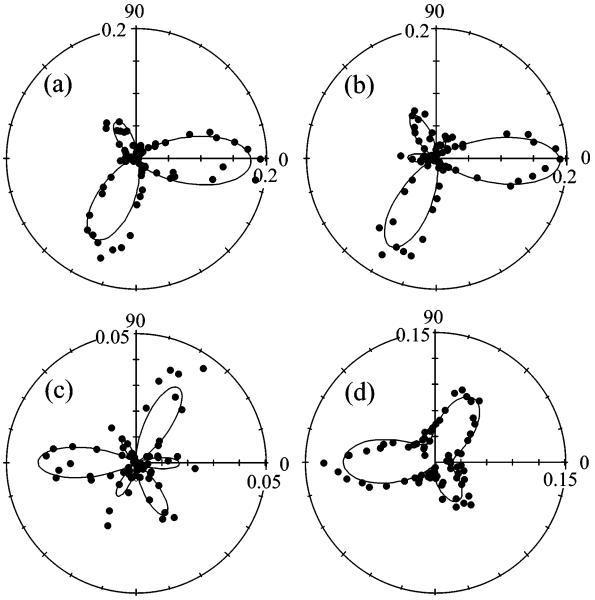

Figure 6. Excitation wavelength dependence of p-in/p-out SH-RA patterns at the Au(643)S surface: (a) 550-nm excitation and 275-nm detection, (b) 580-nm excitation and 290-nm detection, (c) 640-nm excitation and 320-nm detection, and (d) 1064-nm excitation and 532-nm detection.

Acknowledgment. This work was partially supported by a Grant-in-Aid for Scientific Research on Priority Areas (417) from the Ministry of Education, Culture, Sports, Science and Technology (MEXT), Japan. This work was also supported by PRESTO of JST (Japan Science and Technology Agency).

Supporting Information Available: Surface structures of Au(11 8 3), Au(15 12 7), and Au(20 17 12). This material is available free of charge via the Internet at http://pubs.acs.org.

JA053724P